Ann. Nucl. Energy, Vol. 20, No. 3, pp. 167–183, 1993
Printed in Great Britain

0306-4549/93 $6.00+0.00
Pergamon Press Ltd

APPLICATION OF STOCHASTIC DIFFUSION THEORY TO THE INTERPRETATION OF THE ^{252}Cf SOURCE-DRIVEN NOISE ANALYSIS METHOD FOR SUBCRITICALITY DETERMINATION

ALISON M. STOLLE†

Department of Nuclear Engineering, University of Michigan, Ann Arbor, MI 48109, U.S.A.

(Received 8 August 1992)

Abstract—The ^{252}Cf source-driven noise analysis (CSDNA) method is an experimental technique, developed by J. T. Mihalczo and his collaborators at Oak Ridge National Laboratory, which makes use of noise analysis to determine the multiplication factor, k, in subcritical multiplying media. In this work, a stochastic diffusion description was used to interpret the CSDNA experiment in an infinite, homogeneous medium in order to shed light on the practicality of this experimental procedure in determining the multiplication factor. By defining such a benchmark problem, an exact solution is obtained for the subcritical multiplication factor in which the locations of the ^{252}Cf source and neutron detectors are explicitly taken into account. The expression relating reactivity to the measured data was found to depend implicitly on k itself. Through a numerical analysis of this expression, certain limiting conditions were identified in which the expression for the reactivity became essentially independent of k, hence demonstrating some possibility for the viability of this technique. However, under more realistic experimental conditions, i.e. for finite systems in which diffusion theory is not applicable, the measurement of the subcritical multiplication factor from the measured data, without extensive transport calculations, becomes doubtful.

1. INTRODUCTION

The ^{252}Cf source-driven noise analysis (CSDNA) method is an experimental technique developed by J. Mihalczo at Oak Ridge National Laboratory (ORNL) which makes use of noise analysis to determine the multiplication factor of subcritical multiplying media (Mihalczo and Pare, 1975). The method has been implemented for the past 15 years by Mihalczo and his collaborators at ORNL for various compositions and geometries with seemingly satisfactory results (Mihalczo *et al.*, 1978, 1986, 1988, 1990; King and Mihalczo, 1983). In recent years, however, a controversy has developed between the ORNL group and others over the correct analytic expression needed to relate the experimental data, the power spectral densities (PSDs) of the outputs of two neutron detectors and a third external source (^{252}Cf) detector, to the desired result, k (Yamane *et al.*, 1986; Difilippo, 1988; Akcasu and Stolle, 1989; Sutton and Doub, 1991). The origin of this controversy has been explained through a careful interpretation of the experiment using the Langevin equation description of fluctuations at the transport level (Akcasu and Stolle, 1991). This close scrutiny of the CSDNA method has, however, led to other more serious questions concerning the viability of this experiment as a means of determining the subcritical multiplication factor from the measured PSDs. In order to address these questions, a one-speed stochastic diffusion theory description is applied in this paper to the interpretation of the CSDNA experiment for an infinite, homogeneous medium containing a point ^{252}Cf source. By defining a benchmark problem in this way, we are able to obtain an exact solution for the multiplication factor, k, in terms of the measured PSDs, which explicitly accounts for the locations of the detectors and the source and the frequency of the measurement. This exact analysis is performed at the expense, however, of crudeness in the treatment of spectral and transport effects. From this solution, we examine the merits and practicality of the CSDNA experiment for determining the subcritical multiplication factor in the idealized infinite reactor limit.

In the CSDNA experiment, the cross power spectral densities (CPSDs) of three detectors, labelled 1, 2 and 3, as well as the auto power spectral density (APSD) of detector 1 are measured. Detector 1 contains a ^{252}Cf

†Present address: Knolls Atomic Power Lab., P.O. Box 1072, Schenectady, NY 12301, U.S.A.

neutron source and exclusively detects the occurrence of a spontaneous ^{252}Cf fissioning event in which multiple neutrons may be produced. Detectors 2 and 3, which can be located either inside or outside of the multiplying medium, respond to the neutron flux in the multiplying system of interest. A frequency-dependent R ratio is constructed from the measured PSDs, $G_{ij}(\omega)$, where $G_{ij}(\omega)$ is the PSD of the outputs of detectors i and j. This PSD $R(\omega)$ ratio is defined as

$$R(\omega) = \frac{G^*_{12}(\omega)G_{13}(\omega)}{G_{11}(\omega)G_{23}(\omega)}, \tag{1}$$

where the asterisk indicates the complex conjugate. In general, $R(\omega)$ is a complex number that depends on the location of the source and detectors. One can show that for a point reactor model, the $R(\omega)$ ratio can be related to the multiplication factor, k, by

$$\frac{1-k}{k} = \frac{C_1 R}{1-C_2 R}, \tag{2}$$

where C_1 and C_2 are constants involving measurable nuclear parameters (Akcasu and Stolle, 1989). In this idealized zero-dimensional model, a measurement of the R ratio would directly yield the criticality of the system. However, in this paper, we will show that a one-speed, diffusion-level interpretation of the CSDNA experiment in an infinite medium can be put into the same form as equation (2), where the coefficient C_1 actually becomes a function of the reactivity being sought.† Hence, a measurement of the R ratio is not then sufficient to determine the reactivity of the medium, as suggested by the point reactor model. However, by examining the behavior of C_1 as a function of the geometry of the detectors and the source as well as the composition of the reactor, we are able to determine certain limiting conditions in the benchmark problem for which this k-dependence is relatively weak, and hence, obtain an explicit solution for k. Details of the numerical studies of the behavior of C_1, as well as concluding remarks about the CSDNA experimental method for subcriticality determination, are presented in this paper.

2. ONE-SPEED LANGEVIN DIFFUSION DESCRIPTION

Consider a nuclear reactor at a constant power level. The neutron number density, $N(\mathbf{x}, t)$, describes the instantaneous number of neutrons of a single speed, $\langle v \rangle$, in a unit spatial volume element at $\mathbf{x}$ and at time t in the reactor, and satisfies the following one-speed, stochastic diffusion equation:‡

$$\frac{\partial N(\mathbf{x}, t)}{\partial t} = -\nabla \cdot \mathbf{J}(\mathbf{x}, t) - a(\mathbf{x})N(\mathbf{x}, t) + S_N(\mathbf{x}, t), \tag{3}$$

where we define $a(\mathbf{x}) = r_a(\mathbf{x}) - \bar{\nu}_f r_f(\mathbf{x})$ such that $r_a(\mathbf{x}) = \langle v \rangle \Sigma_a(\mathbf{x})$ is the probability per unit time that a neutron is absorbed at $\mathbf{x}$, $r_f(\mathbf{x}) = \langle v \rangle \Sigma_f(\mathbf{x})$ is the rate of induced fission events at $\mathbf{x}$ and $\bar{\nu}_f$ equals the mean number of neutrons produced in an induced fission event. The source term, $S_N(\mathbf{x}, t)$, is a stochastic quantity accounting for the random nature of the capture, fission and external source events occurring in the reactor. In equation (3), $\mathbf{J}(\mathbf{x}, t)$ is the instantaneous diffusion current, and can be represented by the following stochastic Fick's law:

$$\mathbf{J}(\mathbf{x}, t) = -D'(\mathbf{x})\nabla N(\mathbf{x}, t) + \mathbf{S}_j(\mathbf{x}, t), \tag{4}$$

where $D'(\mathbf{x}) = \langle v \rangle D(\mathbf{x})$ and $D(\mathbf{x}) = 1/(3\Sigma_{tr}(\mathbf{x}))$ is the neutron diffusion coefficient. The random nature of the current density is expressed in equation (4) in terms of the stochastic source, $\mathbf{S}_j(\mathbf{x}, t)$. The mean neutron number density satisfies the steady-state diffusion equation

†More generally, a transport-level analysis of the CSDNA experiment is shown to exhibit this k-dependence in the coefficient C_1 in equation (2) (Sutton and Doub, 1991; Akcasu and Stolle, 1991).

‡For the sake of clarity, we ignore delayed neutrons in the one-speed Langevin diffusion equation description of fluctuations, since the effect of delayed neutrons on the interpretation of the CSDNA experiment is not controversial. A space- and velocity-dependent Langevin description of neutron number density fluctuations in the presence of delayed neutrons was first obtained by Akcasu and Osborn (1966), and is applied to the interpretation of the CSDNA experiment by Stolle (1991).

$$a(\mathbf{x})\langle N(\mathbf{x})\rangle + \nabla\cdot\langle \mathbf{J}(\mathbf{x})\rangle = \langle S_{\text{ext}}(\mathbf{x})\rangle, \tag{5}$$

where the mean neutron current density is defined by

$$\langle \mathbf{J}(\mathbf{x})\rangle = -D'(\mathbf{x})\nabla\langle N(\mathbf{x})\rangle. \tag{6}$$

The mean quantities in equations (5) and (6) imply averages over the stochastic sources. Since the ensemble average of equation (3) should reduce to equation (5), the mean of the stochastic source term in equation (3) must equal the mean value of the external source of neutrons, i.e.

$$\langle S_N(\mathbf{x}, t)\rangle = \langle S_{\text{ext}}(\mathbf{x})\rangle. \tag{7}$$

Similarly, from equations (4) and (6), it is apparent that

$$\langle \mathbf{S}_j(\mathbf{x}, t)\rangle = \mathbf{0}. \tag{8}$$

Fluctuations about the mean of the stochastic quantities of interest can now be introduced as

$$n(\mathbf{x}, t) = N(\mathbf{x}, t) - \langle N(\mathbf{x})\rangle, \tag{9a}$$

$$\mathbf{j}(\mathbf{x}, t) = \mathbf{J}(\mathbf{x}, t) - \langle \mathbf{J}(\mathbf{x})\rangle, \tag{9b}$$

$$s_N(\mathbf{x}, t) = S_N(\mathbf{x}, t) - \langle S_{\text{ext}}(\mathbf{x})\rangle \tag{9c}$$

and

$$\mathbf{s}_j(\mathbf{x}, t) = \mathbf{S}_j(\mathbf{x}, t), \tag{9d}$$

and, by subtracting equations (5) and (6) from equations (3) and (4), respectively, we arrive at the following diffusion-level Langevin equation description of neutron number density fluctuations:

$$\frac{\partial n(\mathbf{x}, t)}{\partial t} = -\nabla\cdot\mathbf{j}(\mathbf{x}, t) - a(\mathbf{x})n(\mathbf{x}, t) + s_N(\mathbf{x}, t) \tag{10}$$

and

$$\mathbf{j}(\mathbf{x}, t) = -D'(\mathbf{x})\nabla n(\mathbf{x}, t) + \mathbf{s}_j(\mathbf{x}, t). \tag{11}$$

The fluctuating source terms, $s_N(\mathbf{x}, t)$ and $\mathbf{s}_j(\mathbf{x}, t)$, accounting for the random nature of the neutron number density and current density, respectively, are referred to as the noise equivalent sources (NESs) in the Langevin equation description of fluctuations.

If we eliminate $\mathbf{j}(\mathbf{x}, t)$ by substitution of the stochastic Fick's law into equation (10), the stochastic neutron continuity equation can now be rewritten as

$$\frac{\partial n(\mathbf{x}, t)}{\partial t} = \nabla\cdot D'(\mathbf{x})\nabla n(\mathbf{x}, t) - a(\mathbf{x})n(\mathbf{x}, t) + g(\mathbf{x}, t), \tag{12}$$

where the fluctuating source term, $g(\mathbf{x}, t)$, is

$$g(\mathbf{x}, t) = s(\mathbf{x}, t) - \nabla\cdot\mathbf{s}_j(\mathbf{x}, t). \tag{13}$$

At this stage, the fluctuations in the neutron number density can be obtained formally by solving equation (12) as

$$n(\mathbf{x}, t) = \int_0^\infty du \exp(-B_{\text{diff}}u)g(\mathbf{x}, t-u), \tag{14}$$

where B_{diff} is the diffusion operator, defined as

$$B_{\text{diff}} = -\nabla\cdot D'(\mathbf{x})\nabla + a(\mathbf{x}). \tag{15}$$

The two-time and two-space-point correlation function of the neutron number density fluctuations, i.e.

$$\phi_{\text{nn}}(\mathbf{x}, \mathbf{x}', \tau) = \langle n(\mathbf{x}, t)n(\mathbf{x}', t+\tau)\rangle, \tag{16}$$

can then be directly expressed in terms of the NES correlation function as

$$\phi_{nn}(\mathbf{x}, \mathbf{x}', \tau) = \int_0^\infty du \int_0^\infty dv \exp[-(uB_{diff} + vB'_{diff})]\phi_{ss}(\mathbf{x}, \mathbf{x}', u-v+\tau), \tag{17}$$

where the operators B_{diff} and B'_{diff} operate on $\mathbf{x}$ and $\mathbf{x}'$, respectively, and the NES correlation function, $\phi_{ss}(\mathbf{x}, \mathbf{x}', \tau)$, is defined as

$$\phi_{ss}(\mathbf{x}, \mathbf{x}', \tau) = \langle g(\mathbf{x}, t) g(\mathbf{x}', t+\tau) \rangle. \tag{18}$$

The calculation of $\phi_{ss}(\mathbf{x}, \mathbf{x}', \tau)$ is the central problem in the implementation of the Langevin equation method, in general. The physics of the problem actually lies in this calculation. Once the NES correlation function is known, one can proceed directly and analyze any diffusion theory problem involving different detector configurations. Akcasu and Stolle (1991) show that the statistical properties of the stochastic source in equation (13) are obtained through a mathematical reduction of the NES correlation function at the transport level. The details of the reduction of the transport-level description to obtain the stochastic diffusion description of neutron number density fluctions will not be repeated here, but involve the following mathematical steps: (a) integrating the transport-level stochastic rate equation and NES correlation function over the neutron speed, leading to the stochastic, one-group, transport-level description of fluctuations; (b) further eliminating angular dependence by a spherical harmonics expansion, leading to a space-dependent, one-group, P_1 approximation; and (c) further simplifying the P_1 approximation by taking the large transport-rate limit and thereby introducing the concept of stochastic Fick's law. Through such a reduction procedure, the correlation function of the NES in equation (18) was subsequently shown to be of the form

$$\langle g(\mathbf{x}, t) g(\mathbf{x}', t') \rangle = \delta(t-t') Q_s(\mathbf{x}, \mathbf{x}'), \tag{19}$$

where

$$Q_s(\mathbf{x}, \mathbf{x}') = \delta(\mathbf{x}-\mathbf{x}')\left[(a(\mathbf{x}) + \overline{\upsilon_f(\upsilon_f - 1)} r_f(\mathbf{x}))\langle N(\mathbf{x})\rangle + \bar{m}^2 \langle S_{ext}(\mathbf{x})\rangle\right] + 2\nabla \cdot \nabla'[D'(\mathbf{x})\langle N(\mathbf{x})\rangle \delta(\mathbf{x}-\mathbf{x}')]. \tag{20}$$

The stochastic diffusion description in equations (12), (19) and (20) provide the necessary mathematical expressions to proceed with the evaluation of the $R(\omega)$ ratio in the CSDNA method for subcriticality determination.

3. DETERMINATION OF THE R(ω) RATIO

Consider an infinite, homogeneous reactor containing a point neutron source and two neutron detectors (2 and 3) at positions $\mathbf{x}_0$, $\mathbf{x}_2$ and $\mathbf{x}_3$, respectively, in the multiplying medium. A third detector (1) exclusively detects the spontaneous fission of ^{252}Cf, the neutron point source located at $\mathbf{x}_0$. Let S_0 represent the mean rate of occurrence of ^{252}Cf source events. The proposed benchmark problem is examined for one-speed neutrons in an infinite medium characterized by the following spatially uniform parameters: r_a, r_f and D'. The detection rate is included in r_a, so that the medium is uniform in the presence of the detector. A steady-state solution to the benchmark problem can be found from equations (5) and (6), where $\langle S_{ext}(x)\rangle = \bar{m} S_0 \delta(\mathbf{x}-\mathbf{x}_0)$. First, we express the mean neutron number density in Fourier space with respect to $\mathbf{x}$ as

$$\langle N(\mathbf{q})\rangle = \frac{\bar{m} S_0 \exp(i\mathbf{q}\cdot\mathbf{x}_0)}{D'\left(q^2 + \dfrac{a}{D'}\right)}, \tag{21}$$

where

$$\langle N(\mathbf{q})\rangle = \int d^3q \exp(-i\mathbf{q}\cdot\mathbf{x})\langle N(\mathbf{x})\rangle, \tag{22}$$

and by performing the inverse Fourier transform on equation (21), we obtain the desired and well-known result

$$\langle N(\mathbf{x})\rangle = \frac{\bar{m}S_0}{4\pi D'} \frac{\exp\left(-\sqrt{\frac{a}{D'}}|\mathbf{x}-\mathbf{x}_0|\right)}{|\mathbf{x}-\mathbf{x}_0|}. \tag{23}$$

We now apply the stochastic Langevin diffusion description to the analysis of the temporal behavior of neutron density fluctuations in this benchmark reactor. A stochastic diffusion description of the CSDNA experiment requires, in addition to the stochastic Langevin equation for fluctuations in the neutron number density, stochastic rate equations describing fluctuations in the accumulated counts in detectors 1, 2, and 3. The fluctuations in the instantaneous detection rate of detector j are defined as

$$i_j(t) = I_j(t) - \langle I_j\rangle, \tag{24}$$

where $\langle I_j\rangle$ represents the mean detection rate in detector j. Hence, the coupled set of Langevin equations become

$$\frac{\partial n(\mathbf{x}, t)}{\partial t} = D'\nabla^2 n(\mathbf{x}, t) - an(\mathbf{x}, t) + g(\mathbf{x}, t), \tag{25}$$

$$i_{D_1}(t) = \int_{V_{D_1}} \mathrm{d}^3x\, s_{D_1}(\mathbf{x}, t) \tag{26}$$

and

$$i_{D_j}(t) = \int_{V_{D_j}} \mathrm{d}^3x[r_{D_j} n(\mathbf{x}, t) + s_{D_j}(\mathbf{x}, t)], \quad j = 2, 3. \tag{27}$$

The detection rate of neutrons in detector j is defined by r_{D_j}. The NES terms, $s_{D_j}(\mathbf{x}, t)$, account for the probabilistic nature of the detection process in detector j. The statistical properties of the NESs appearing in equations (25)–(27) must be known in order to analyze the benchmark problem. Equations (19) and (20) define the NES correlation function for $g(\mathbf{x}, t)$. In addition, the following correlation functions are needed in this analysis:

$$\langle s_{D_1}(\mathbf{x}, t) g(\mathbf{x}', t')\rangle = \delta(t-t') p_1 \bar{m} S_0 \delta(\mathbf{x}-\mathbf{x}_0)\delta(\mathbf{x}-\mathbf{x}') \tag{28}$$

and

$$\langle g(\mathbf{x}, t) s_{D_j}(\mathbf{x}', t')\rangle = -\delta(t-t')\delta(\mathbf{x}-\mathbf{x}') r_{D_j}\langle N(\mathbf{x})\rangle. \tag{29}$$

A derivation of these correlation functions is provided by Stolle (1991). Here, it is assumed that a neutron is removed upon detection. We now proceed to an exact determination of the $R(\omega)$ ratio by directly evaluating its defining quantities: $G_{11}(\omega)$, $G_{12}(\omega)$, $G_{13}(\omega)$ and $G_{23}(\omega)$.

The ASPD of detector 1, $G_{11}(\omega)$, is determined by applying a random point process procedure described by Akcasu and Stolle (1991). In this reference, the APSD for the output of detector 1 is directly determined by treating the fluctuations in the rate of ^{252}Cf source events as a Poisson impulse process (shot noise treatment). The details of these calculations are not repeated, instead the results are simply restated here as

$$G_{11}(\omega) = p_1 S_0. \tag{30}$$

Next, we proceed with the evaluation of the CPSD between the ^{252}Cf source detector (1) and neutron detector j ($j = 2, 3$). Starting with stochastic rate equations (26) and (27) for fluctuations in the detection rate, the correlation function for the outputs of source detector 1 and neutron detector j becomes

$$\begin{aligned}\langle i_{D_1}(t) i_{D_j}(t')\rangle &= \int_{V_{D_1}} \mathrm{d}^3x \int_{V_{D_j}} \mathrm{d}^3x' r_{D_j}\langle s_{D_1}(\mathbf{x}, t) n(\mathbf{x}', t')\rangle \\ &= \phi_{1j}(t, t'),\end{aligned} \tag{31}$$

where we have implemented the relationship

$$\langle s_{D_i}(\mathbf{x}, t) s_{D_j}(\mathbf{x}', t')\rangle = 0 \quad \text{for} \quad i \neq j \quad \text{(different detectors)}, \tag{32}$$

a statement of the uncorrelated nature of the NES terms for the outputs of two different detectors. Hence, the determination of the desired CPSD, $G_{1j}(\omega)$, is reduced to evaluating the correlation function $\langle s_{D_1}(\mathbf{x}, t)n(\mathbf{x}', t')\rangle$ in equation (31). At this stage in our CPSD calculations, as well as in the following calculations performed to evaluate $G_{23}(\omega)$, mathematical manipulations are simplified and certain cancellations become more apparent by working in Fourier space with respect to both time, t, and space, $\mathbf{x}$. Neutron number density fluctuations in Fourier space are defined as follows:

$$\tilde{n}(\mathbf{q}, \omega) = \int_{-\infty}^{\infty} dt \exp(i\omega t) \int d^3x \exp(i\mathbf{q}\cdot\mathbf{x}) n(\mathbf{x}, t). \tag{33}$$

If we now take the Fourier transform of the stochastic rate equation (25) with respect to space and time, $\tilde{n}(\mathbf{q}, \omega)$ can be expressed in terms of its Fourier-transformed NES as

$$\tilde{n}(\mathbf{q}, \omega) = \frac{\tilde{g}(\mathbf{q}, \omega)}{D'\left(q^2 + \dfrac{a + i\omega}{D'}\right)}. \tag{34}$$

The determination of the correlation function $\langle s_{D_1}(\mathbf{x}, t)n(\mathbf{x}', t')\rangle$ in equation (31) can now be transformed into the evaluation of the correlation function of the NESs in $(\mathbf{q}, \omega)$ space, i.e. we take the Fourier transform of the stochastic rate equations (26) and (27) with respect to t and t', respectively, such that

$$\begin{aligned}\langle i_{D_1}(\omega) i_{D_j}(\omega')\rangle &= \int_{V_{D_1}} d^3x \int_{V_{D_j}} d^3x' \, r_{D_j} \langle s_{D_1}(\mathbf{x}, \omega) n(\mathbf{x}', \omega')\rangle \\ &= \int_{V_{D_1}} d^3x \int_{V_{D_j}} d^3x' \, r_{D_j} \left[\frac{1}{(2\pi)^3}\right]^2 \int d^3q \int d^3q' \exp[-(\mathbf{q}\cdot\mathbf{x} + \mathbf{q}'\cdot\mathbf{x}')] \frac{\langle s_{D_1}(\mathbf{q}, \omega) g(\mathbf{q}', \omega')\rangle}{D'\left(q'^2 + \dfrac{a + i\omega}{D'}\right)}.\end{aligned} \tag{35}$$

The relationship of the correlated function $\langle i_{D_1}(\omega) i_{D_j}(\omega')\rangle$ to the desired CPSD, $G_{1j}(\omega)$, is not immediately obvious, but can be shown by returning to the definition of the CPSD:

$$\begin{aligned}G_{1j}(\omega) &= \int_{-\infty}^{\infty} d\tau \exp(i\omega\tau) \langle i_{D_1}(t) i_{D_j}(t+\tau)\rangle \\ &= \int_{-\infty}^{\infty} d\tau \exp(i\omega\tau) r_{D_j} \int_{V_{D_1}} d^3x \int_{V_{D_j}} d^3x' \langle s_{D_1}(\mathbf{x}, t) n(\mathbf{x}', t+\tau)\rangle.\end{aligned} \tag{36}$$

Here, the CPSD, $G_{1j}(\omega)$, is defined above by the Fourier transform of the current–current correlation function $\langle i_{D_1}(t) i_{D_j}(t+\tau)\rangle$ with respect to the time difference, τ, whereas the current–current correlation function in equation (35), equated in terms of the correlation function of the NESs, is derived by Fourier transforming the stochastic rate equations for current fluctuations in detector 1 and j with respect to t and t' ($t' = t + \tau$), respectively. A relationship between equations (35) and (36) is developed by utilizing our general knowledge of stationary Markov processes. That is, we recognize that the correlation function, $\phi_{1j}(t, t')$, in equation (31), for a stationary Markov process is a function of $t' - t = \tau$. Employing this property, we say

$$\begin{aligned}\langle i_{D_1}(\omega) i_{D_j}(\omega')\rangle &= \int_{-\infty}^{\infty} dt \int_{-\infty}^{\infty} dt' \exp(-i\omega t) \langle i_{D_1}(t) i_{D_j}(t')\rangle \exp(-i\omega' t') \\ &= \int_{-\infty}^{\infty} dt \int_{-\infty}^{\infty} dt' \exp[-i(\omega t + \omega' t')] \phi_{1j}(t' - t) \\ &= \int_{-\infty}^{\infty} d\tau \exp(i\omega\tau) \phi_{1j}(\tau) \int_{-\infty}^{\infty} dt' \exp[-i(\omega + \omega')t'] \\ &= 2\pi\delta(\omega + \omega') G_{1j}(\omega).\end{aligned} \tag{37}$$

The statistical properties of the NESs are also a function of this time difference [see equations (28) and (29)]. Performing similar mathematical maneuvers to those above, we write

$$\langle s_{D_1}(\mathbf{x},\omega)g(\mathbf{x}',\omega')\rangle = \int_{-\infty}^{\infty} dt \int_{-\infty}^{\infty} dt' \exp(-i\omega t)\langle s_{D_1}(\mathbf{x},t)g(\mathbf{x}',t')\rangle \exp(-i\omega' t')$$

$$= p_1 \bar{m} S_0 \delta(\mathbf{x}-\mathbf{x}_0)\delta(\mathbf{x}-\mathbf{x}') \int_{-\infty}^{\infty} dt \int_{-\infty}^{\infty} dt' \exp[-i(\omega t+\omega' t')]\delta(t-t')$$

$$= p_1 \bar{m} S_0 \delta(\mathbf{x}-\mathbf{x}_0)\delta(\mathbf{x}-\mathbf{x}')2\pi\delta(\omega+\omega'). \tag{38}$$

From equations (35), (37) and (38), we are now able to express $G_{1j}(\omega)$ by

$$G_{1j}(\omega) = \int_{V_{D_1}} d^3x \int_{V_{D_j}} d^3x' r_{D_j} \frac{1}{(2\pi)^3} \int d^3q' \exp(-i\mathbf{q}'\cdot\mathbf{x}') \frac{p_1 \bar{m} S_0 \delta(\mathbf{x}-\mathbf{x}_0)\exp(-i\mathbf{q}'\cdot\mathbf{x}_0)}{D'\left(q'^2+\dfrac{a-i\omega}{D'}\right)}, \tag{39}$$

where we have transformed equation (38) into $\mathbf{q},\mathbf{q}'$ space and integrated over all $\mathbf{q}$. Equation (39) immediately reduces to

$$G_{1j}(\omega) = \frac{p_1 \bar{m} S_0}{4\pi D'} r_{D_j} \int_{V_{D_j}} d^3x' \frac{\exp\left(-\sqrt{\dfrac{a-i\omega}{D'}}\,|\mathbf{x}-\mathbf{x}_0|\right)}{|\mathbf{x}-\mathbf{x}_0|}, \tag{40}$$

such that we obtain the desired solution for the CPSD for the outputs of source detector 1 and neutron detector j. We emphasize here that equation (40) is exact. Results are obtained from the Langevin diffusion theory description directly applied to the infinite benchmark reactor under consideration. The limitations of equation (40) arise only in connection with the applicability of diffusion theory to adequately model neutron behavior in the system, and hence is not an issue in our benchmark problem solution.

The determination of the CPSD between the outputs of neutron detectors 2 and 3 proceeds in much the same fashion as the evaluation of $G_{1j}(\omega)$. Stochastic rate equation (27) provides us with the cross-correlation function describing neutron detector current fluctuations as

$$\langle i_{D_2}(t) i_{D_3}(t')\rangle = \int_{V_{D_2}} d^3x \int_{V_{D_3}} d^3x' [r_{D_2} r_{D_3}\langle n(\mathbf{x},t)n(\mathbf{x}',t')\rangle + r_{D_2}\langle n(\mathbf{x},t)s_{D_3}(\mathbf{x}',t')\rangle + r_{D_3}\langle s_{D_2}(\mathbf{x},t)n(\mathbf{x}',t')\rangle]. \tag{41}$$

Correlation functions on the right-hand side of equation (41) are expressible directly in terms of the NES correlation functions, and mathematical simplifications are very straightfoward by again proceeding in $\mathbf{q},\mathbf{q}',\omega,\omega'$ space. Thus, in light of these observations, the CPSD between the outputs of detectors 2 and 3 becomes

$$G_{23}(\omega) = \int_{-\infty}^{\infty} d\tau \exp(-i\omega\tau)\langle i_{D_2}(t) i_{D_3}(t+\tau)\rangle$$

$$= \int_{V_{D_2}} d^3x \int_{V_{D_3}} d^3x' \frac{1}{(2\pi)^6} \int d^3q \int d^3q' \exp(-i\mathbf{q}\cdot\mathbf{x})\exp(-i\mathbf{q}'\cdot\mathbf{x}')$$

$$\times \left[r_{D_2} r_{D_3} \frac{\langle \tilde{g}(\mathbf{q},\omega)\tilde{g}^*(\mathbf{q}',\omega)\rangle}{D'^2\left(q^2+\dfrac{a+i\omega}{D'}\right)\left(q'^2+\dfrac{a-i\omega}{D'}\right)} + r_{D_2} \frac{\langle \tilde{g}(\mathbf{q}',\omega)\tilde{s}^*_{D_2}(\mathbf{q},\omega)\rangle}{D'\left(q^2+\dfrac{a+i\omega}{D'}\right)} + r_{D_3} \frac{\langle \tilde{s}_{D_2}(\mathbf{q},\omega)\tilde{g}^*(\mathbf{q}',\omega)\rangle}{D'\left(q'^2+\dfrac{a-i\omega}{D'}\right)} \right]. \tag{42}$$

The transformation of NES properties into $\mathbf{q},\mathbf{q}'$ space is performed is a straightforward manner. From equation (20), the NES correlation function in $\mathbf{q},\mathbf{q}'$ space can easily be determined to be

$$\langle \tilde{g}(\mathbf{q},\omega)\tilde{g}^*(\mathbf{q}',\omega)\rangle = [a+\overline{\upsilon_f(\upsilon_f-1)}r_f]\bar{N}(\mathbf{q}+\mathbf{q}')+\overline{m^2}S_0\exp[i(\mathbf{q}+\mathbf{q}')\cdot\mathbf{x}_0]-2D'(\mathbf{q}\cdot\mathbf{q}')\bar{N}(\mathbf{q}+\mathbf{q}'). \quad (43)$$

The two remaining NES correlation functions in equation (42) are also transformed to $\mathbf{q},\mathbf{q}'$ space such that

$$\langle \tilde{g}(\mathbf{q},\omega)\tilde{s}^*_{D_3}(\mathbf{q}',\omega)\rangle = -r_{D_3}\bar{N}(\mathbf{q}+\mathbf{q}') \quad (44a)$$

and

$$\langle \tilde{s}_{D_2}(\mathbf{q},\omega)\tilde{g}^*(\mathbf{q}',\omega)\rangle = -r_{D_2}\bar{N}(\mathbf{q}+\mathbf{q}'). \quad (44b)$$

Inserting equations (43), (44a) and (44b) into equation (42), the following expression remains to be simplified:

$$G_{23}(\omega) = \int_{V_{D_2}} d^3x \int_{V_{D_3}} d^3x' \, r_{D_2}r_{D_3} \frac{1}{(2\pi)^6}\int d^3q \int d^3q' \exp(-i\mathbf{q}\cdot\mathbf{x})\exp(-i\mathbf{q}'\cdot\mathbf{x}')$$

$$\times\left\{\frac{\overline{m^2}S_0\exp[i(\mathbf{q}+\mathbf{q}')\cdot\mathbf{x}_0]+[a+\overline{\upsilon_f(\upsilon_f-1)}r_f-2D'\mathbf{q}\cdot\mathbf{q}']\bar{N}(\mathbf{q}+\mathbf{q}')}{D'^2\left(q^2+\dfrac{a+i\omega}{D'}\right)\left(q'^2+\dfrac{a-i\omega}{D'}\right)}\right.$$

$$\left.-\left[\frac{1}{D'\left(q^2+\dfrac{a+i\omega}{D'}\right)}+\frac{1}{D'\left(q'^2+\dfrac{a-i\omega}{D'}\right)}\right]\bar{N}(\mathbf{q}+\mathbf{q}')\right\}. \quad (45)$$

By acquiring a common denominator, immediate cancellations occur whereby

$$G_{23}(\omega) = \int_{V_{D_2}} d^3x \int_{V_{D_3}} d^3x' \frac{1}{(2\pi)^6}\int d^3q \exp(-i\mathbf{q}\cdot\mathbf{x})\int d^3q' \exp(-i\mathbf{q}'\cdot\mathbf{x}')\frac{r_{D_2}r_{D_3}}{D'^2\left(q^2+\dfrac{a+i\omega}{D'}\right)\left(q'^2+\dfrac{a-i\omega}{D'}\right)}$$

$$\times\left[\overline{m^2}S_0\exp[i(\mathbf{q}+\mathbf{q}')\cdot\mathbf{x}_0]+\overline{\upsilon_f(\upsilon_f-1)}r_f\bar{N}(\mathbf{q}+\mathbf{q}')-D'\left(q^2+q'^2+2\mathbf{q}\cdot\mathbf{q}'+\frac{a}{D'}\right)\bar{N}(\mathbf{q}+\mathbf{q}')\right]. \quad (46)$$

By inserting the Fourier-transformed function $\bar{N}(\mathbf{q}+\mathbf{q}')$, which is defined in equation (21), into equation (46), and performing further simplifications, we find that

$$G_{23}(\omega) = \int_{V_{D_2}} d^3x \int_{V_{D_3}} d^3x' \frac{1}{(2\pi)^6}\int d^3q \exp(-i\mathbf{q}\cdot\mathbf{x})\int d^3q' \exp(-i\mathbf{q}'\cdot\mathbf{x}')r_{D_2}r_{D_3}$$

$$\times\frac{\overline{m(m-1)}S_0\exp[i(\mathbf{q}+\mathbf{q}')\cdot\mathbf{x}_0]+\overline{\upsilon_f(\upsilon_f-1)}r_f\bar{N}(\mathbf{q}+\mathbf{q}')}{D'^2\left(q^2+\dfrac{a+i\omega}{D'}\right)\left(q'^2+\dfrac{a-i\omega}{D'}\right)}. \quad (47)$$

The above inverse Fourier transformations are performed so that we arrive at the following final expression for the CPSD of the outputs of neutron detectors 2 and 3:

$$G_{23}(\omega) = \int_{V_{D_2}} d^3x \int_{V_{D_3}} d^3x' \, r_{D_2}r_{D_3}\left[\frac{\overline{\upsilon_f(\upsilon_f-1)}r_f\bar{m}S_0}{(4\pi D')^3}J(\mathbf{x},\mathbf{x}',\omega)\right.$$

$$\left.+\frac{\overline{m(m-1)}S_0}{(4\pi D')^2}\frac{\exp\left(-\sqrt{\dfrac{a+i\omega}{D'}}|\mathbf{x}-\mathbf{x}_0|\right)}{|\mathbf{x}-\mathbf{x}_0|}\frac{\exp\left(-\sqrt{\dfrac{a-i\omega}{D'}}|\mathbf{x}'-\mathbf{x}_0|\right)}{|\mathbf{x}'-\mathbf{x}_0|}\right], \quad (48)$$

where

$$J(\mathbf{x},\mathbf{x}',\omega)=\int \mathrm{d}^3z \frac{\exp\left(-\sqrt{\frac{a}{D'}}z\right)}{z}\frac{\exp\left(-\sqrt{\frac{a+i\omega}{D'}}|\mathbf{x}-\mathbf{z}|\right)}{|\mathbf{x}-\mathbf{z}|}\frac{\exp\left(-\sqrt{\frac{a-i\omega}{D'}}|\mathbf{x}'-\mathbf{z}|\right)}{|\mathbf{x}'-\mathbf{z}|}. \tag{49}$$

Notice that equations (40) and (48) are essentially a Green's function for the CPSD $G_{1j}(\omega)$ and $G_{23}(\omega)$, since these expressions are derived for a point source at $\mathbf{x}_0$.

We now introduce one assumption into our thus far exact analysis before putting the R ratio in its final form. Evaluating equations (40) and (48) for the CPSDs $G_{1j}(\omega)$ and $G_{23}(\omega)$, respectively, requires integration over neutron detector volumes. We will now examine these expressions in the small detector limit. In this limit, we assume the integrands in equations (40) and (48) remain constant over the detector volume with that constant value determined by evaluating each integrand at the location of the center of the neutron detector volume over which the integration is performed. Reducing the CPSD expressions in this small detector limit, we present our final results as

$$G_{11}(\omega)=p_1S_0, \tag{50}$$

$$G_{12}(\omega)=\frac{r_{D_2}p_1\bar{m}S_0V_{D_2}}{4\pi D'}\frac{\exp\left(-\sqrt{\frac{a-i\omega}{D'}}|\mathbf{x}_2|\right)}{|\mathbf{x}_2|}, \tag{51}$$

$$G_{13}(\omega)=\frac{r_{D_3}p_1\bar{m}S_0V_{D_3}}{4\pi D'}\frac{\exp\left(-\sqrt{\frac{a-i\omega}{D'}}|\mathbf{x}_3|\right)}{|\mathbf{x}_3|} \tag{52}$$

and

$$G_{23}(\omega)=r_{D_2}r_{D_3}V_{D_2}V_{d_3}\left[\frac{\overline{\upsilon_f(\upsilon_f-1)}r_f\bar{m}S_0}{(4\pi D')^3}J(\mathbf{x}_2,\mathbf{x}_3,\omega)\right.$$
$$\left.+\frac{\overline{m(m-1)}S_0}{(4\pi D')^2}\frac{\exp\left(-\sqrt{\frac{a+i\omega}{D'}}|\mathbf{x}_2|\right)}{|\mathbf{x}_2|}\frac{\exp\left(-\sqrt{\frac{a-i\omega}{D'}}|\mathbf{x}_3|\right)}{|\mathbf{x}_3|}\right], \tag{53}$$

where we now have assumed that the ^{252}Cf point source and detector 1 are located at the origin, without any loss of generality.

As a final step, the resulting expressions for $G_{11}(\omega)$, $G_{12}(\omega)$, $G_{13}(\omega)$ and $G_{23}(\omega)$ are inserted into the definition of R in equation (1) to obtain the final form for the ratio of PDSs as

$$R=\frac{p_1\bar{m}^2}{\overline{m(m-1)}+\overline{\upsilon_f(\upsilon_f-1)}r_f\bar{m}\left[\frac{1}{4\pi D'}|\mathbf{x}_2||\mathbf{x}_3|\exp(\lambda|\mathbf{x}_2|)\exp(\lambda^*|\mathbf{x}_3|)J(\mathbf{x}_2,\mathbf{x}_3,\omega)\right]}, \tag{54}$$

where

$$\lambda=\sqrt{\frac{a+i\omega}{D'}}\quad\text{and}\quad\lambda^*=\sqrt{\frac{a-i\omega}{D'}}.$$

Hence, equation (54) is an exact diffusion theory solution to the theoretical determination of R for the infinite, homogeneous benchmark reactor. The form of equation (54) contains explicit dependence on the spatial location of the neutron source and detectors in its description of R. In addition, the R ratio is shown also to be a function of the frequency, ω, of the measurement. However, despite its complicated appearance, notice the striking similarities that exist between equation (54) and the R ratio expression for a point reactor, a form previously determined to be (Akcasu and Stolle, 1989):

$$R = \frac{p_1 \bar{m}^2}{\overline{m(m-1)} + \overline{\upsilon_f(\upsilon_f - 1)} r_f \bar{m} \dfrac{1}{a}}. \tag{55}$$

We now wish to utilize the similarities in equations (54) and (55) noted above and attempt to cast the R ratio for the benchmark reactor into the point form expression for the multiplication factor expressed in equation (2), where the, as yet, undetermined coefficients will now contain space- and frequency-dependent terms. How we extract the reactivity from the involved expression for the R ratio in equation (54) is not altogether apparent. The k_∞ dependence is buried in the exponential terms in equation (54), where we note that parameter $a = r_a(1-k_\infty)$. Hence, an explicit solution for k_∞ is essentially impossible. However, we find that the point form expression for system criticality in equation (2) can be achieved if coefficient C_1 is itself allowed to contain k_∞ dependence. To demonstrate how this point form is obtained, we must rewrite the function

$$Y(\mathbf{x}_2, \mathbf{x}_3, k_\infty, \omega) = \frac{1}{4\pi D'} |\mathbf{x}_2||\mathbf{x}_3| \exp(\lambda|\mathbf{x}_2|) \exp(\lambda^*|\mathbf{x}_3|) J(\mathbf{x}_2, \mathbf{x}_3, k_\infty, \omega) \tag{56}$$

in terms of new, "scaled" parameters

$$\mathbf{y}_2 = \sqrt{\frac{a}{D'}}\,\mathbf{x}_2, \tag{57}$$

$$\mathbf{y}_3 = \sqrt{\frac{a}{D'}}\,\mathbf{x}_3, \tag{58}$$

$$\mathbf{z}' = \sqrt{\frac{a}{D'}}\,\mathbf{z} \tag{59}$$

$$\lambda' = \frac{\lambda}{\sqrt{\dfrac{a}{D'}}} = \sqrt{1 + i\frac{\omega}{a}} = \sqrt{1 + i\omega'}; \quad \omega' = \frac{\omega}{a} \tag{60}$$

such that equation (56) becomes

$$Y(\mathbf{x}_2, \mathbf{x}_3, k_\infty, \omega) = \frac{1}{a} I(\mathbf{x}_2, \mathbf{x}_3, k_\infty, \omega), \tag{61}$$

where

$$I(\mathbf{x}_2, \mathbf{x}_3, k_\infty, \omega) = \frac{1}{4\pi} |\mathbf{y}_2||\mathbf{y}_3| \exp(\lambda'|\mathbf{y}_2|) \exp(\lambda'^*|\mathbf{y}_3|) \int \mathrm{d}^3 z' \frac{\exp(-z')}{z'} \frac{\exp(-\lambda'|\mathbf{y}_2 - \mathbf{z}'|)}{|\mathbf{y}_2 - \mathbf{z}'|} \frac{\exp(-\lambda'^*|\mathbf{y}_3 - \mathbf{z}'|)}{|\mathbf{y}_3 - \mathbf{z}'|}. \tag{62}$$

Although we have done nothing more than rewrite the function $Y(\mathbf{x}_2, \mathbf{x}_3, k_\infty, \omega)$, the $1/a$ factor that arises in equation (61) by the parametric substitution above in equations (57)–(60) allows us to cast equation (54) into an expression for k_∞ in the desired point form. That is, by substituting equation (61) into equation (54), we find

$$\frac{1-k_\infty}{k_\infty} = \frac{\dfrac{1}{p_1 \bar{m}} \left(\dfrac{\overline{\upsilon_f^2}}{\overline{\upsilon_f}} - 1 \right) I(\mathbf{x}_2, \mathbf{x}_3, k_\infty, \omega) R}{1 - \dfrac{1}{p_1 \bar{m}} \left(\dfrac{\overline{m^2}}{\bar{m}} - 1 \right) R}, \tag{63}$$

where, from equation (2) it is apparent that

$$C_1 = \frac{1}{p_1 \bar{m}} \left(\frac{\overline{v_f^2}}{\bar{v}_f} - 1 \right) I(\mathbf{x}_2, \mathbf{x}_3, k_\infty, \omega) \tag{64}$$

and

$$C_2 = \frac{1}{p_1 \bar{m}} \left(\frac{\overline{m^2}}{\bar{m}} - 1 \right). \tag{65}$$

What explicitly have we accomplished by rewriting equation (54) in the form of equation (63) above? The statement of equality in equations (54) and (63) is obviously the same. A defining equation for the subcritical multiplication factor is not achieved, since a k_∞-dependent function itself would exist in the definition. However, if closer examination into the k_∞ behavior of $I(\mathbf{x}_2, \mathbf{x}_3, k_\infty, \omega)$ provides certain limiting conditions for which this k_∞-dependence is relatively weak, a technique unfolds in which an experimentally measured R ratio can be used to evaluate system criticality through an expression involving known nuclear and geometrical parameters. In other words, application of the CSDNA method for the determination of the subcritical multiplication factor could then be justified for the benchmark reactor under investigation, while the effects of neutron source and detector locations are now explicitly accounted for by a spatial correction factor to the point model. Therefore, we now proceed with a parametric investigation into the numerical behavior of $I(\mathbf{x}_2, \mathbf{x}_3, k_\infty, \omega)$.

4. NUMERICAL ANALYSIS AND DISCUSSION OF RESULTS

Any further comments regarding the applicability of the CSDNA technique to the determination of reactivity first requires, at this stage in our benchmark analysis, an investigation into the numerical behavior of I as a function of neutron detector locations, $\mathbf{x}_2$ and $\mathbf{x}_3$, the multiplication factor, k_∞, and the measurement frequency, ω, where

$$I(\mathbf{x}_2, \mathbf{x}_3, k_\infty, \omega) = \frac{1}{4\pi} |\mathbf{y}_2||\mathbf{y}_3| \exp(\lambda'|\mathbf{y}_2|) \exp(\lambda'^*|\mathbf{y}_3|) \int d^3z' \frac{\exp(-z')}{z'} \frac{\exp(-\lambda'|\mathbf{y}_2 - \mathbf{z}'|)}{|\mathbf{y}_2 - \mathbf{z}'|} \frac{\exp(-\lambda'^*|\mathbf{y}_3 - \mathbf{z}'|)}{|\mathbf{y}_3 - \mathbf{z}'|} \tag{66}$$

and the scaled parameters are defined in equations (57)–(60). Of particular significance in this study is identifying certain limiting cases or parametric regions, i.e. neutron detector locations, in which the k_∞ dependence of I becomes, for all practical purposes, negligible. Under such limiting conditions, we have shown that the CSDNA method for k_∞ determination for this idealized benchmark reactor can be implemented by utilizing equation (63).

Simplifications were introduced into equation (66) by considering a colinear detector–source–detector configuration in the infinite medium. Numerical calculations were then performed under three different sets of assumptions. First, we examined the behavior of I, and in turn R, as a function of both detector distance from the source and reactivity for neutron detectors equidistant from the source. The calculations for equally-spaced detectors were again divided into two subcategories. In Case 1, the measurement frequency was taken to be 0, while ω was allowed to vary in Case 2. Finally, the complex nature of the function I was exhibited in Case 3 by allowing detectors 2 and 3 to be unequally positioned from the source in the colinear configuration and by introducing a non-zero measurement frequency into the calculations. Each of the cases described here is now presented in turn below with numerical results shown graphically.

Case 1

The first set of numerical calculations were executed by considering colinear neutron detectors at equal distance from the source and for $\omega = 0$. Under this set of assumptions, we find that the following mathematical simplifications occur:

$$\lambda' = 1, \quad |\mathbf{y}_2| = |\mathbf{y}_3| = |\mathbf{y}| = y,$$

where $y = \sqrt{(a/D')}x$ and x is the magnitude of the distance of the neutron detectors from the source. In addition, we notice

$$|\mathbf{y}_2-\mathbf{z}| = |\mathbf{y}_3-\mathbf{z}| = y^2+z^2-2yz\mu,$$

where $\mu = \cos\theta$. Introducing these simplifications into equation (66), one finds

$$I(y) = y^2 \exp(2y) \int_0^\infty dz\, z \exp(-z) \int_0^1 d\mu \frac{\exp\left[-\alpha\left(\sqrt{1-\varepsilon\mu}+\sqrt{1+\varepsilon\mu}\right)\right]}{\alpha^2\sqrt{1-\varepsilon^2\mu^2}}, \tag{67}$$

where

$$\varepsilon = \frac{2yz}{y^2+z^2} \quad \text{and} \quad \alpha = \sqrt{y^2+z^2}.$$

The set of assumptions made in Case 1 reduced the form of I to a function of the single parameter, y, now requiring only double integration. The parameter, y, a function of both detector distance and system criticality, can be rewritten in terms of the neutron diffusion length as

$$y = \sqrt{\frac{a}{D'}}x = \frac{x}{L_{\text{diff}}}\sqrt{1-k_\infty}.$$

Hence, the value of y is a measure of the number of diffusion lengths the detectors are placed from the source for a given k_∞. Numerical results were obtained for $I(y)$ as a function of y by employing a numerical integration scheme available in the packaged software *Mathematica* (Wolfram, 1988). All numerical calculations were performed on the Macintosh personal computer. Figures 1–8 present graphically our numerical findings for Case 1.

In Fig. 1, $I(y)$ is plotted as a function of the parameter y. The numerical results show $I(y)$ to be a non-decreasing function of y which initially demonstrates a relatively rapid increase followed by a leveling off or plateauing of the function for large values. This asymptotic behavior of $I(y)$ can be predicted by examining equation (67) in the large y limit. That is,

$$\lim_{y\to\infty} I(y) = \lim_{y\to\infty} \left\{ y^2 \exp(2y) \int_0^\infty dz\, z \exp(-z) \int_0^1 d\mu \frac{\exp\left[-\sqrt{y^2+z^2}\left(\sqrt{1-\frac{2yz}{y^2+z^2}\mu}+\sqrt{1+\frac{2yz}{y^2+z^2}\mu}\right)\right]}{(y^2+z^2)\sqrt{1-\frac{4y^2z^2}{y^2+z^2}\mu^2}} \right\}$$

$$\to y^2 \exp(2y) \int_0^\infty dz\, z \exp(-z) \int_0^1 d\mu \frac{\exp(-2y)}{y^2}$$

$$\to \int_0^\infty dz\, z \exp(-z) = 1.$$

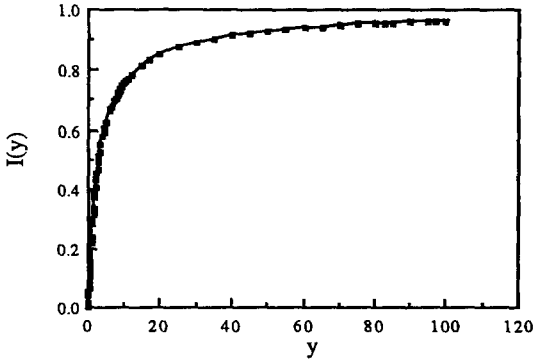

Fig. 1. I as a function of the parameter y.

The numerical results reflect this asymptotic limit since $I(y)$ is seen to approach 1 for increasing values of y. In general, large y values correspond to highly subcritical systems with neutron detectors located many diffusion lengths from the source. However, we utilize our numerical results [$I(y)$ vs y] to examine these trends in more detail by studying the effects of k_∞ and x/L_{diff} separately.

For several fixed values of k_∞, the behavior of I and R as a function of x/L_{diff} is shown in Figs 2 and 3. As expected, increasing subcriticality from 0.95 to k_∞ values of 0.75 and 0.5 for any given x/L_{diff}, i.e. a trend which translates directly into increasing y, produces increasing values of I. All three curves in Fig. 2 approach an asymptotic limit of 1; however, when k_∞ is close to critical ($k_\infty = 1$), very large values of x/L_{diff} are required to approach this asymptotic limit. On the other hand, an increase in I for a given k_∞ reflects a decrease in the value of R, demonstrated in Fig. 3. The asymptotic behavior of I leads to an asymptotic limit for R for large values of x/L_{diff}, a limit easily shown to be

$$R = \frac{p_1 \bar{m}^2}{\overline{m(m-1)} + \dfrac{\overline{\upsilon_f(\upsilon_f - 1)}}{\bar{\upsilon}_f} \bar{m} \dfrac{k_\infty}{1 - k_\infty}}.$$

Nuclear parameters used in this numerical study were assigned the following values

$$p_1 = 1, \qquad \bar{\upsilon}_f = 2.408,$$

$$\bar{m} = 3.773, \qquad \frac{\overline{\upsilon_f(\upsilon_f - 1)}}{\bar{\upsilon}_f^2} = 0.8,$$

$$\overline{m^2} = 15.818.$$

For a given detector configuration, we now investigate the behavior of I and R as a function of k_∞. In this study, maximum values of I occur at $k_\infty = 0$, such that $I_{\max} = I(x/L_{\text{diff}})$. This behavior is shown in Fig. 4. Predictably, larger values of I are reflected for larger values of x/L_{diff} for any fixed k_∞. The corresponding R behavior is plotted in Fig. 5. Here we notice that for $k_\infty = 0$

$$R = \frac{p_1 \bar{m}^2}{\overline{m(m-1)}} = 1.1819,$$

irregardless of neutron detector locations. Figure 4 also sheds light on the applicability of the CSDNA technique to determine the subcriticality of the infinite reactor under investigation. For a system configuration which positions neutron detectors far from the point source, especially for $x/L_{\text{diff}} \geqslant 100$, $I(k_\infty)$ remains essentially a constant for a large range of k_∞ values. Therefore, in the experimental determination of R would translate directly into system criticality through equation (63) with a constant value for I equal to $I(x/L_{\text{diff}})$.

The effort to account for spatial effects in our benchmark reactor requires both extensive theoretical analysis to obtain an exact solution for the R ratio and numerical calculations to evaluate R. Therefore, we are led to an inevitable question, especially if we view equation (63) from an experimental standpoint. How well can the

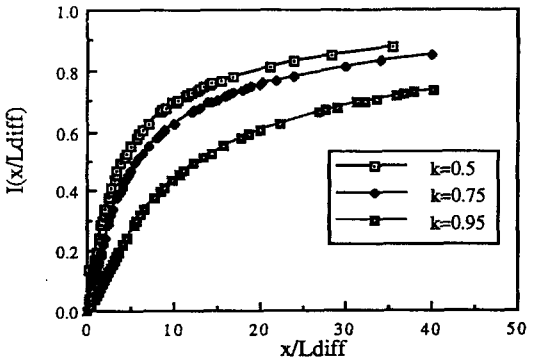

Fig. 2. I as a function of x/L_{diff} for $k = 0.5$, 0.75 and 0.95.

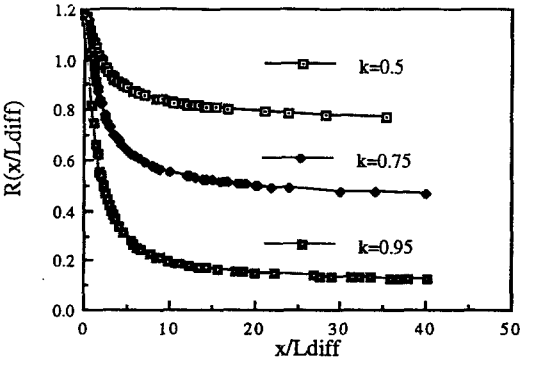

Fig. 3. R as a function of x/L_{diff} for $k = 0.5$, 0.75 and 0.95.

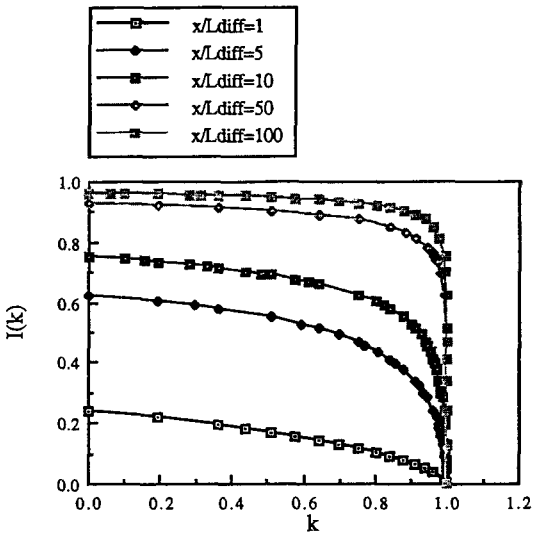

Fig. 4. I as a function of k for $x/L_{\text{diff}} = 1, 5, 10, 50$ and 100.

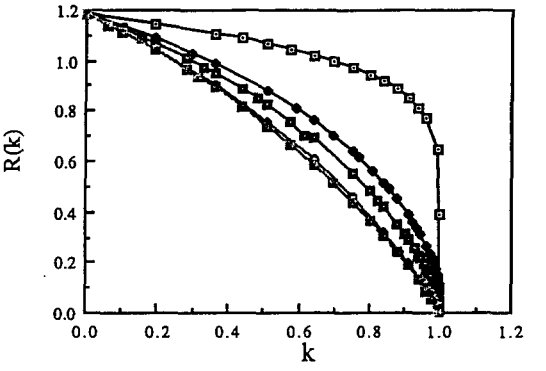

Fig. 5. R as a function of k for $x/L_{\text{diff}} = 1, 5, 10, 50$ and 100. Symbols as in Fig. 4.

multiplication factor be predicted for the infinite, homogeneous reactor by employing a simple point reactor model? From Akcasu and Stolle (1989), a point reactor model of the CSDNA experiment corresponds to $I = 1$ in equation (63). We extend the definition of the point reactor model here to include any constant value for I, not necessarily equal to 1. In Figs 6–8, we present exact results for R as a function of k_∞ given different detector locations. In addition, for each detector configuration, we attempt to fit several point model solutions to the exact behavior of k_∞. The constant values of I are chosen such that $R_{\text{pt}} = R_{\text{exact}}$ for several fixed values of k_∞. A comparison is also performed for $I = 1$. For neutron detectors placed at 1 and 5 diffusion lengths from the source, Figs 6 and 7 demonstrate the crudeness of the fitted point solution and thus, the strong presence of spatial effects. However, as the detectors are positioned farther from the source, spatial effects

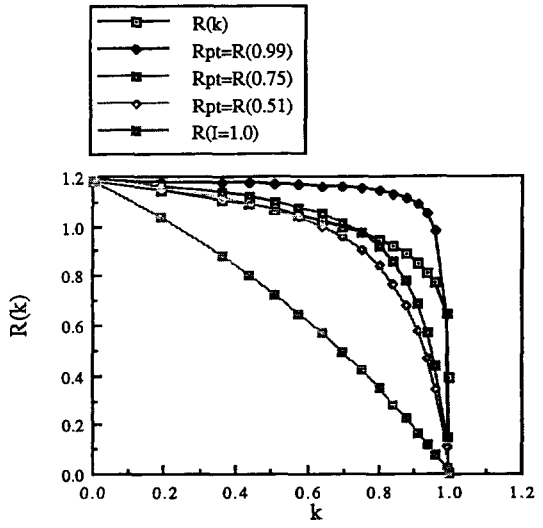

Fig. 6. Point model of space-dependent problem, $x/L_{\text{diff}} = 1$.

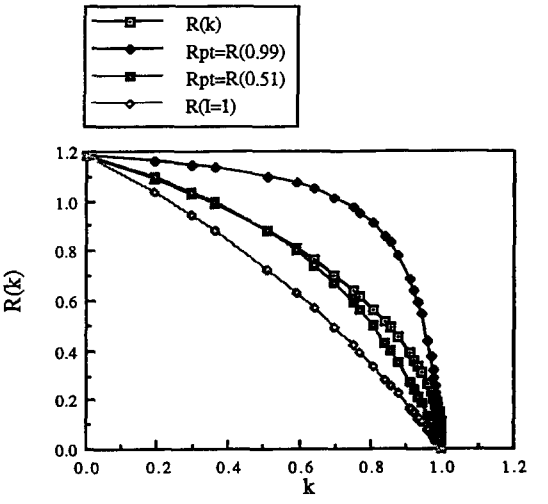

Fig. 7. Point model of space-dependent problem, $x/L_{\text{diff}} = 5$.

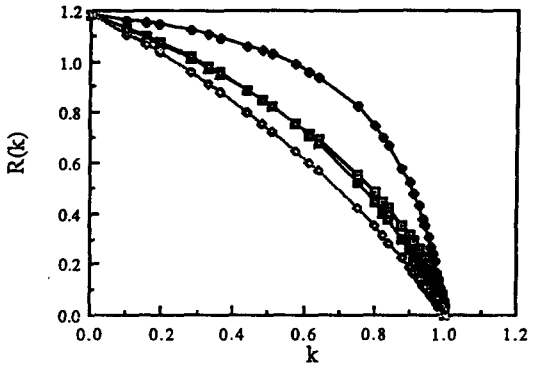

Fig. 8. Point model of space-dependent problem, $x/L_{\text{diff}} = 10$.

become negligible, as evidenced in Fig. 8. Results are presented in this figure for detectors at 10 diffusion lengths from the source, where the exact solution becomes almost indistinguishable from a fitted point solution.

Case 2

In general, the functional form of I includes a dependency on the measurement frequency, ω. We examine this dependency for the colinear detector–source–detector arrangement and now perform numerical calculations for

$$I(y) = \tfrac{1}{2}y^2 \exp\left[(\lambda' + \lambda'^*)y\right] \int_0^\infty dz\, z \exp(-z) \int_{-1}^{1} d\mu \frac{\exp\left[-\alpha(\lambda'\sqrt{1-\varepsilon\mu} + \lambda'^*\sqrt{1+\varepsilon\mu})\right]}{\alpha^2\sqrt{1-\varepsilon^2\mu^2}} \tag{68}$$

as a function of the variable, ω, where, as noted earlier,

$$\lambda' = \sqrt{1+i\omega'} = \sqrt{1+i\frac{\omega}{a}}.$$

These numerical results are acquired by considering the benchmark reactor with equally-spaced neutron detectors at 20 diffusion lengths from the source and a system criticality of $k_\infty = 0.75$. Through this numerical study, we discover that I suffers an initial rapid decline which tapers off as $I \to 0$ for increasing values of ω. A corresponding asymptotic limit is approached by R as this increasing function tends to

$$R \to \frac{p_1 \bar{m}^2}{m(m-1)} = 1.1819$$

for increasing values of the frequency. These findings are displayed in Figs 9 and 10. Worthy of mention here

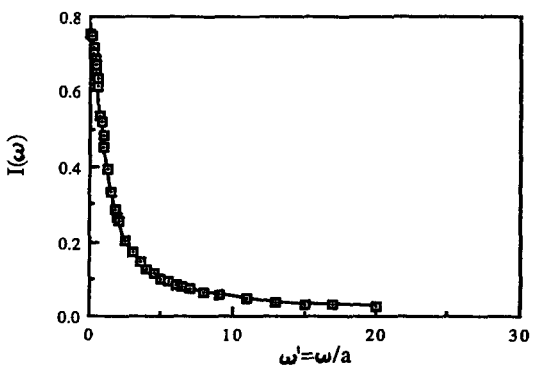

Fig. 9. I as a function of ω' for $x/L_{\text{diff}} = 20$ and $k = 0.75$.

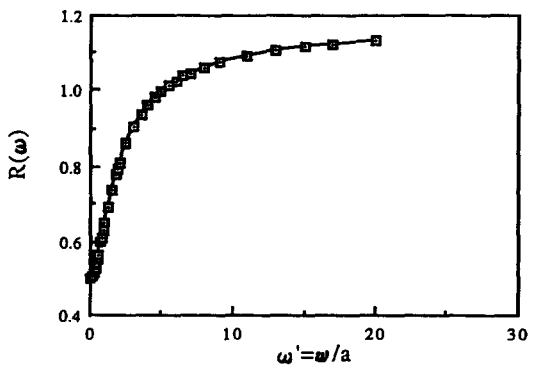

Fig. 10. R as a function of ω' for $x/L_{\text{diff}} = 20$ and $k = 0.75$.

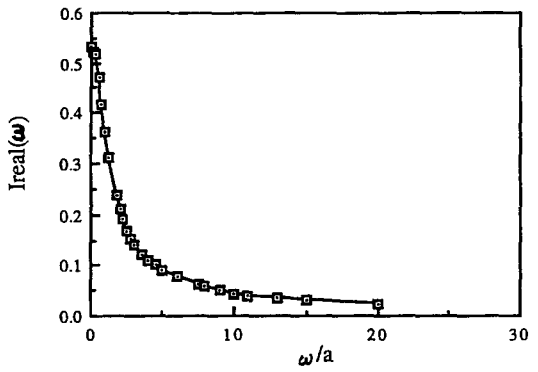

Fig. 11. Real part of I as a function of ω for $x_2/L_{\text{diff}} = 5$, $x_3/L_{\text{diff}} = 10$ and $k = 0.75$.

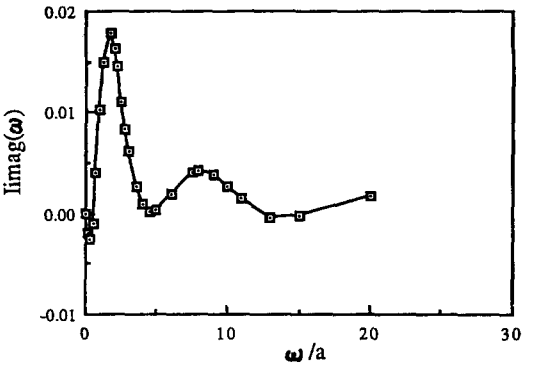

Fig. 12. Imaginary part of I as a function of ω for $x_2/L_{\text{diff}} = 5$, $x_3/L_{\text{diff}} = 10$ and $k = 0.75$.

is the complex nature of the function I. For colinear detectors at equal distance from the source, we find the values of I to be purely real. However, this observation leads us to our third and final case study of the numerical behavior of I.

Case 3

The complex nature of I is exhibited for non-zero ω when we analyze the colinear detector–source–detector system for neutron detectors which are unequally positioned from the source. Under these circumstances, equation (66) reduces to

$$I(y) = \tfrac{1}{2} y_2 y_3 \exp(\lambda' y_2 + \lambda'^* y_3) \int_0^\infty dz\, z \exp(-z) \int_{-1}^{1} d\mu \frac{\exp\left(-\alpha_2 \lambda' \sqrt{1-\varepsilon_2 \mu} - \alpha_3 \lambda'^* \sqrt{1+\varepsilon_3 \mu}\right)}{\alpha_2 \alpha_3 \sqrt{1-\varepsilon_2 \mu}\sqrt{1+\varepsilon_3 \mu}}. \quad (69)$$

where

$$y_2 = |\mathbf{y}_2| = \frac{x_2}{L_{\text{diff}}}\sqrt{1-k_\infty}; \quad \varepsilon_2 = \frac{2y_2 z}{y_2^2 + z^2}$$

and

$$y_3 = |\mathbf{y}_3| = \frac{x_3}{L_{\text{diff}}}\sqrt{1-k_\infty}; \quad \varepsilon_3 = \frac{2y_3 z}{y_3^2 + z^2}$$

and x_2 and x_3 define the distance of neutron detectors from the source. Both real and imaginary components of I are plotted as a function of ω in Figs 11 and 12, where the numbers reflect a reactor with $k_\infty = 0.75$, $x_2/L_{\text{diff}} = 5$ and $x_3/L_{\text{diff}} = 10$. Due to the differences in the relative magnitudes of the real and imaginary components of I, the sinusoidal features displayed in Fig. 12 representing the imaginary behavior of I are not reflected in the graphical representation of $|I(\omega)|$, the magnitude of the function, presented in Fig. 13.

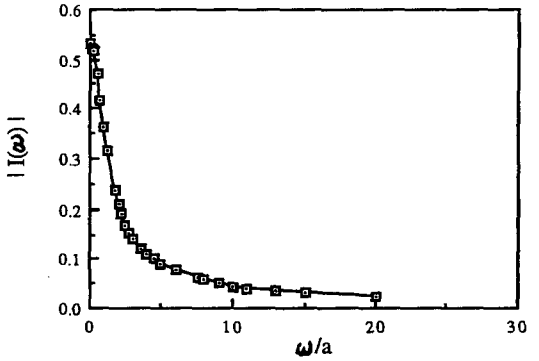

Fig. 13. Magnitude of I as a function of ω for $x_2/L_{\text{diff}} = 5$, $x_3/L_{\text{diff}} = 10$ and $k = 0.75$.

5. CONCLUSIONS

Through a theoretical and numerical investigation of the CSDNA technique for the defined benchmark reactor, we obtain an exact expression in equation (63) relating the $R(\omega)$ ratio to the subcritical multiplication factor of the reactor. In the previous section, the function I was found to be relatively insensitive to k_∞, for a wide range of k_∞ values if a colinear detector–source–detector configuration was implemented for detectors far from the source and equally spaced. Under these conditions, the reactivity can be determined from an experimental R value without prior knowledge of k_∞ to determine I. Applying equation (63) to the investigation of the CSDNA experiment for a realistic reactor configuration, however, may not accurately predict the reactivity if the experimental conditions are far from the benchmark conditions considered. However, under more realistic experimental conditions, i.e. for finite systems in which diffusion theory is not applicable, the determination of the subcritical multiplication factor from a single measured ratio of PSDs without extensive transport calculations, becomes doubtful.

Obtaining an exact expression for the R ratio becomes increasingly complicated as the sophistication of the physical reactor model increases. In addition, Langevin diffusion theory may eventually need to be discarded for a more realistic treatment of neutron behavior, such as the P_1, one-speed transport, or even complete transport Langevin descriptions. Eventually, one may encounter a situation in which a detailed theoretical description of the experimental set-up is achieved, but that the corresponding set of equations becomes essentially impossible to solve. How may the measured R ratio then be utilized to evaluate the unknown reactivity for an arbitrary system?

From our benchmark studies, we discover some evidence to support the use of a calibration curve in the determination of k from the measured R ratio. In particular, by employing a colinear detector–source–detector configuration such that detectors are placed far from the source, I may become relatively insensitive to the properties of the infinite medium. Thus, using equation (63) and a constant value for I, we may immediately plot k_∞ as a function of R. By maintaining the same source–detectors configuration, a measured R ratio might then translate directly into the subcritical multiplication factor of the system from such a calibation curve for any medium which meets the infinite medium description.

In general, one needs to determine the reactivity of a finite, space-dependent multiplying medium. For a fixed geometrical configuration, between the point source, finite medium and neutron detectors, a calibration curve can be evaluated using Monte Carlo calculations. If the same geometrical configuration is then maintained, and assuming we can extrapolate from our benchmark reactor analysis, this calibration curve may possibly be used to interpret a measured R ratio to determine the multiplication factor of an unknown medium.

As a final remark, some of the results obtained, such as the high-frequency limit of $R(\omega)$, and conclusions reached in this paper using the benchmark problem may be due to the use of the diffusion approximation and the infinite medium model. The benchmark problem, in which spatial effects are now included in the expression for $R(\omega)$, should be considered as one step beyond the point model. The correct limiting behavior of $R(\omega)$ or k_∞ should, in general, be investigated at the transport level using the general results presented previously by Stolle (1991).

REFERENCES

Akcasu A. Z. and Osborn R. K. (1966) *Nucl. Sci. Engng* **26,** 13.
Akcasu A. Z. and Stolle A. M. (1989) *Ann. Nucl. Energy* **16,** 493.
Akcasu A. Z. and Stolle A. M. (1991) *Trans. Am. Nucl. Soc.* **64,** 300.
Difilippo F. C. (1988) *Nucl. Sci. Engng* **99,** 28.
King W. T. and Mihalczo J. T. (1983) *Trans. Am. Nucl. Soc.* **44,** 290.
Mihalczo J. T. and Pare V. K. (1975) *Ann. Nucl. Energy* **2,** 97.
Mihalczo J. T., Pare V. K., Ragan G. L., Mathis M. V. and Tillett G. C. (1978) *Nucl. Sci. Engng* **66,** 29.
Mihalczo J. T., Kryter R. C., King W. T. and Blakeman E. D. (1986) *Ann. Nucl. Energy* **13,** 351.
Mihalczo J. T., Blakeman E. D. and Ragan G. E. (1988) *Trans. Am. Nucl. Soc.* **57,** 133.
Mihalczo J. T., Blakeman E. D., Ragan G. E. and Johnson E. B. (1990) *Nucl. Sci. Engng* **104,** 314.
Stolle A. M. (1991) Anatomy of a controversy: application of the Langevin technique to the analysis of the ^{252}Cf source-driven noise analysis method for subcriticality determination. Ph.D. Thesis, Dept of Nuclear Engineering, Univ. of Michigan, Ann Arbor, MI.
Sutton T. and Doub W. B. (1991) *Ann. Nucl. Energy* **18,** 491.
Williams M. M. R. (1974) *Random Processes in Nuclear Reactors.* Pergamon Press, New York.
Wolfram S. (1988) *Mathematica.* Addison-Wesley, Reading, MA.
Yamane Y., Watanabe S., Nishina K., Miyoshi Y., Suzaki T. and K-Bayashi I. (1986) *J. At. Energy Soc. Japan* **28**(9), 850.